







# Targeting RUNX1 as a novel treatment modality for pulmonary arterial hypertension

Euy-Myoung Jeong <sup>1†</sup>, Mandy Pereira <sup>1,2†</sup>, Eui-Young So<sup>1</sup>, Keith Q. Wu<sup>1</sup>, Michael Del Tatto <sup>1</sup>, Sicheng Wen <sup>1</sup>, Mark S. Dooner <sup>1</sup>, Patrycja M. Dubielecka<sup>1</sup>, Anthony M. Reginato<sup>3</sup>, Corey E. Ventetulo<sup>2</sup>, Peter J. Quesenberry<sup>1</sup>, James R. Klinger<sup>2</sup>, and Olin D. Liang <sup>1\*</sup>

<sup>1</sup>Division of Hematology/Oncology, Department of Medicine, Rhode Island Hospital, Warren Alpert Medical School of Brown University, Providence, RI 02903, USA; <sup>2</sup>Division of Pulmonary, Critical Care and Sleep Medicine, Department of Medicine, Rhode Island Hospital, Warren Alpert Medical School of Brown University, Providence, RI 02903, USA; and <sup>3</sup>Division of Rheumatology, Department of Medicine, Rhode Island Hospital, Warren Alpert Medical School of Brown University, Providence, RI 02903, USA

Received 9 June 2020; editorial decision 14 December 2021; accepted 6 January 2022; online publish-ahead-of-print 9 January 2022

Time for primary review: 35 days

## Aims

Pulmonary arterial hypertension (PAH) is a fatal disease without a cure. Previously, we found that transcription factor RUNX1-dependent haematopoietic transformation of endothelial progenitor cells may contribute to the pathogenesis of PAH. However, the therapeutic potential of RUNX1 inhibition to reverse established PAH remains unknown. In the current study, we aimed to determine whether RUNX1 inhibition was sufficient to reverse Sugen/hypoxia (SuHx)-induced pulmonary hypertension (PH) in rats. We also aimed to demonstrate possible mechanisms involved.

## Methods and results

We administered a small molecule specific RUNX1 inhibitor Ro5-3335 before, during, and after the development of SuHx-PH in rats to investigate its therapeutic potential. We quantified lung macrophage recruitment and activation *in vivo* and *in vitro* in the presence or absence of the RUNX1 inhibitor. We generated conditional VE-cadherin-CreERT2; ZsGreen mice for labelling adult endothelium and lineage tracing in the SuHx-PH model. We also generated conditional Cdh5-CreERT2; Runx1(flox/flox) mice to delete *Runx1* gene in adult endothelium and LysM-Cre; Runx1(flox/flox) mice to delete *Runx1* gene in cells of myeloid lineage, and then subjected these mice to SuHx-PH induction. RUNX1 inhibition *in vivo* effectively prevented the development, blocked the progression, and reversed established SuHx-induced PH in rats. RUNX1 inhibition significantly dampened lung macrophage recruitment and activation. Furthermore, lineage tracing with the inducible VE-cadherin-CreERT2; ZsGreen mice demonstrated that a RUNX1-dependent endothelial to haematopoietic transformation occurred during the development of SuHx-PH. Finally, tissue-specific deletion of *Runx1* gene either in adult endothelium or in cells of myeloid lineage prevented the mice from developing SuHx-PH, suggesting that RUNX1 is required for the development of PH.

## Conclusion

By blocking RUNX1-dependent endothelial to haematopoietic transformation and pulmonary macrophage recruitment and activation, targeting RUNX1 may be as a novel treatment modality for pulmonary arterial hypertension.

## Keywords

Endothelial cells • Macrophages • RUNX1 • Pulmonary hypertension

\*Corresponding author. Tel: 617-816-8885; fax: 401-444-2486, E-mail: olin\_liang@brown.edu

†The first two authors contributed equally to this study.

© The Author(s) 2022. Published by Oxford University Press on behalf of the European Society of Cardiology.

This is an Open Access article distributed under the terms of the Creative Commons Attribution-NonCommercial License (<https://creativecommons.org/licenses/by-nc/4.0/>), which permits non-commercial re-use, distribution, and reproduction in any medium, provided the original work is properly cited. For commercial re-use, please contact [journals.permissions@oup.com](mailto:journals.permissions@oup.com)

## 1. Introduction

Pulmonary arterial hypertension (PAH) is a rare but progressive disease without a cure. The hallmark of PAH is the development of pulmonary vascular remodelling, which leads to elevated pulmonary vascular resistance, right heart failure, and ultimately death.<sup>1–3</sup> Current therapies that consist of drugs with selective pulmonary vasodilatory properties can improve symptoms and delay disease progression, but their disease modifying effects are minimal.<sup>4,5</sup> There is a critical need to develop novel treatments that target the underlying cause of the pulmonary vascular remodelling in PAH.

A strong association of PAH with dysregulated immunity and inflammation has been well-established. Considerable data have accrued to suggest that perivascular inflammatory responses mediated by bone marrow (BM)-derived macrophages play a primary role in the pathogenesis of PAH.<sup>6,7</sup> Thus, evaluation of novel therapies for PAH that target both the origin and the activation of macrophages is warranted. Runt-related transcription factor 1 (RUNX1) is a member of the core-binding factor family of transcription factors that is indispensable for embryonic endothelial to haematopoietic transition (EHT) and the establishment of definitive haematopoiesis in vertebrates.<sup>8–10</sup> RUNX1 partners with a constitutively expressed  $\beta$  subunit (core-binding factor  $\beta$ ; CBF $\beta$ ) to form a transcriptionally active heterodimer that can either activate or repress target gene expression.<sup>11</sup> Mice with a homozygous knockout of *Runx1* lack definitive haematopoiesis and are unable to survive past an early embryonic stage (Days 11.5–12.5).<sup>12</sup> In our previous study, specific inhibition of RUNX1 blocked egress of BM-derived endothelial progenitor cells (EPCs) and attenuated the development of pulmonary hypertension (PH) in mice.<sup>13</sup> We postulate that RUNX1 is required in the myeloid-skewed haematopoietic transformation of BM-derived EPCs during the development of PAH. In support of this hypothesis, we found that gene expression of *Runx1* is increased in circulating CD34 + CD133 + EPCs isolated from peripheral blood of patients with PH.<sup>13</sup>

Macrophages that mediate inflammation have been classified as M1, whereas those that resolve inflammation as M2 macrophages.<sup>14</sup> Our earlier studies showed that the drastic increases in production of pro-inflammatory cytokines (e.g. IL-1 $\beta$ , IL-6, and TNF- $\alpha$ ) and chemokines (e.g. fractalkine/CX3CL1 and MCP-1/CCL2) attributed to M1 macrophages and M1 macrophage-treated endothelial cells (ECs) coincide with the elevated levels of the same cytokines and chemokines found in PAH patients.<sup>15</sup> It is possible that M1 macrophages are the mediators of perivascular inflammation leading to pulmonary vascular remodelling. Interestingly, direct binding of RUNX1 to p50-NF- $\kappa$ B in macrophages was shown to trigger signals responsible for production of pro-inflammatory cytokines.<sup>16,17</sup> Taken together, we hypothesize that RUNX1 plays a pivotal role in the production and activation of macrophages that lead to perivascular inflammation and vascular remodelling in PAH. To test this hypothesis, we inhibited RUNX1 activity via a small molecule specific inhibitor Ro5-3335<sup>18</sup> and examined its effect on overall macrophage production, recruitment, and activation, and the attenuation of PH in the Sugen/hypoxia (SuHx) rat model. Our objectives were to determine whether inhibition of RUNX1 was sufficient to reverse established PH and to also determine possible mechanisms involved. The current report is an extension of previously published work by our group which described that inhibition of RUNX1 prevents development of SuHx-induced PH in mice.<sup>13</sup> In the present study, we now show that RUNX1 inhibition is not only effective in mice but also in rats, which is the more established model to investigate PAH. Furthermore, we show that inhibition of RUNX1 does not only prevent but also reverses SuHx-

PH in rats. In addition, we generated transgenic mice with deletion of *Runx1* gene in adult endothelium or in cells of myeloid lineage. We found that the tissue-specific *Runx1* deficiency protects the mice from developing SuHx-PH, indicating that RUNX1 is required for the development of PH. Overall, our study suggests that, by blocking RUNX1-dependent endothelial to haematopoietic transformation and pulmonary macrophage recruitment and activation, targeting RUNX1 may be as a novel treatment modality for PAH.

## 2. Methods

### 2.1 SuHx-PH model in rats

The SuHx-PH model in rats was carried out as published previously,<sup>19</sup> which is also described in detail in [Supplementary material online](#). Rats were anaesthetized via isoflurane inhalation (1–3%). For euthanasia, the inferior vena cava was transected and the anaesthetized rats were euthanized by exsanguination. All animal experiments were approved by the Lifespan Institutional Animal Care and Use Committee (IACUC) at Rhode Island Hospital. All procedures were performed conforming to the NIH Guide for the Care and Use of Laboratory Animals.

### 2.2 Study protocols of RUNX1 inhibition *in vivo*

A prevention, an intervention, and a reversal protocol were used in this study. In the disease prevention protocol, rats were given 20 mg/kg of Ro5-3335 in 100  $\mu$ L of DMSO or 100  $\mu$ L vehicle alone by subcutaneous injection every other day for three times at the beginning of SuHx treatment, and the development of PH was assessed 1 week after removal from hypoxia (Hx) (*Figure 1A*). In the disease intervention protocol, rats were given 20 mg/kg of Ro5-3335 in 100  $\mu$ L of DMSO or 100  $\mu$ L vehicle alone by subcutaneous injection every other day for three times 1 week after the beginning of SuHx treatment, and the development of PH was assessed 1 week after removal from Hx (*Figure 3A*). In the disease reversal protocol, rats were given 20 mg/kg of Ro5-3335 in 100  $\mu$ L of DMSO or 100  $\mu$ L vehicle alone by subcutaneous injection every other day for six times after the completion of SuHx treatment, and the development of PH was assessed 2 weeks after removal from Hx (*Figure 4A*). Bronchoalveolar lavage (BAL) fluid of the rats was collected by inserting a catheter in the trachea, through which 5 mL phosphate buffered saline (PBS) was instilled into the bronchioles and the BAL fluid was gently retracted. After centrifugation, the BAL supernatants were frozen at –20°C and used later to detect inflammatory cytokines. The cell pellets were resuspended in PBS and treated with the Red Blood Cell Lysis Buffer (MilliporeSigma, Burlington, MA) followed by twice PBS washes and filtration through a nylon mesh. Cells in the BAL fluid were fixed and permeabilized with LEUCOPERM (Bio-Rad, Hercules, CA) and stained with a mouse monoclonal antibody against rat CD68 conjugated with Alexa Fluor 488 (clone ED1, Bio-Rad) to identify rat macrophages. Flow cytometry analysis was performed on a 4-laser LSR II flow cytometer (BD Biosciences, San Diego, CA) and data were analysed with the FlowJo software (FlowJo, Ashland, OR).

### 2.3 Histologic analysis of lung sections

Histologic analysis of lung sections were carried out as described in [Supplementary material online](#).

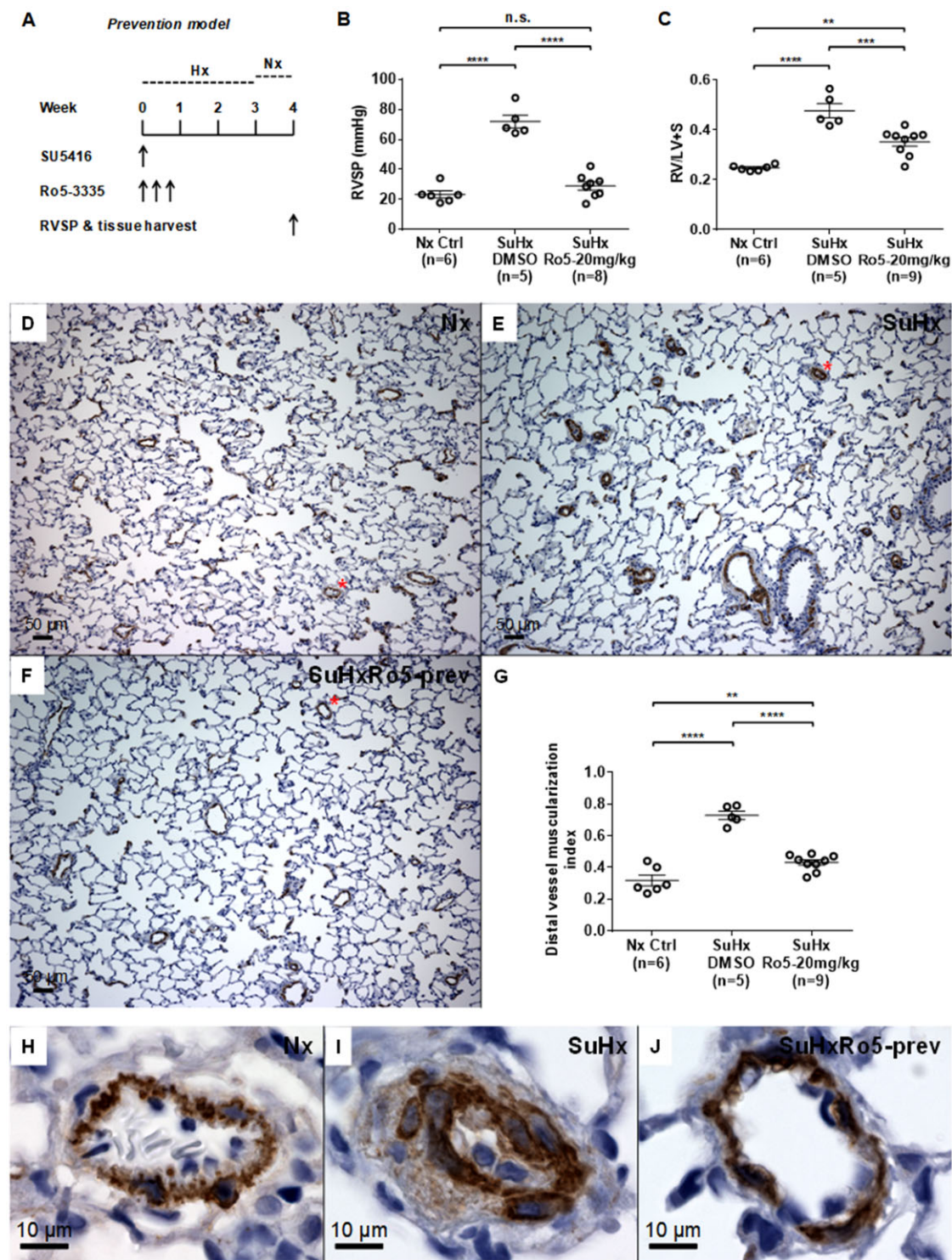


**Figure 1** Inhibition of RUNX1 *in vivo* prevents the development of SuHx/hypoxia-induced pulmonary hypertension (SuHx-PH) in rats. (A) Experimental protocol for prevention of SuHx-PH in rats shows administration of the RUNX1 inhibitor Ro5-3335 (Ro5) every other day for three times at the beginning of SuHx treatment. SU5416: VEGF receptor 2 antagonist Sugen 5416. (B and C) Right ventricular systolic pressure (RVSP) (B) and the Fulton's index (right ventricle to left ventricle + septum, RV/LV+S ratio) (C) were measured 1 week after removal from 3 weeks of hypoxia (Hx). (D–F) Representative microscopic images of 100× magnification show immunohistochemical (IHC) staining in brown colour of  $\alpha$ -smooth muscle actin ( $\alpha$ -SMA) in the blood vessels from lungs of normoxia control (Nx Ctrl) rats (D), vehicle DMSO-treated SuHx rats (E), and 20 mg/kg Ro5-treated SuHx rats (F). (G) Muscularization of distal pulmonary vessels less than 50  $\mu$ m in diameter was assessed by calculating the muscularization index defined as the total area of the vessel that stained positive for  $\alpha$ -SMA divided by total cross-sectional area of the vessel. (H–J) Representative small blood vessels stained in brown colour of  $\alpha$ -SMA, which are labelled with a red asterisk in (D–F), are shown in 600× magnification: (H) Nx Ctrl rats; (I) vehicle DMSO-treated SuHx rats; and (J) Ro5-treated SuHx rats. \*\* $P < 0.01$ , \*\*\* $P < 0.001$ , \*\*\*\* $P < 0.0001$ , n.s.: not significant, ordinary one-way ANOVA with multiple comparisons,  $n$  = number of animals in each experimental group.

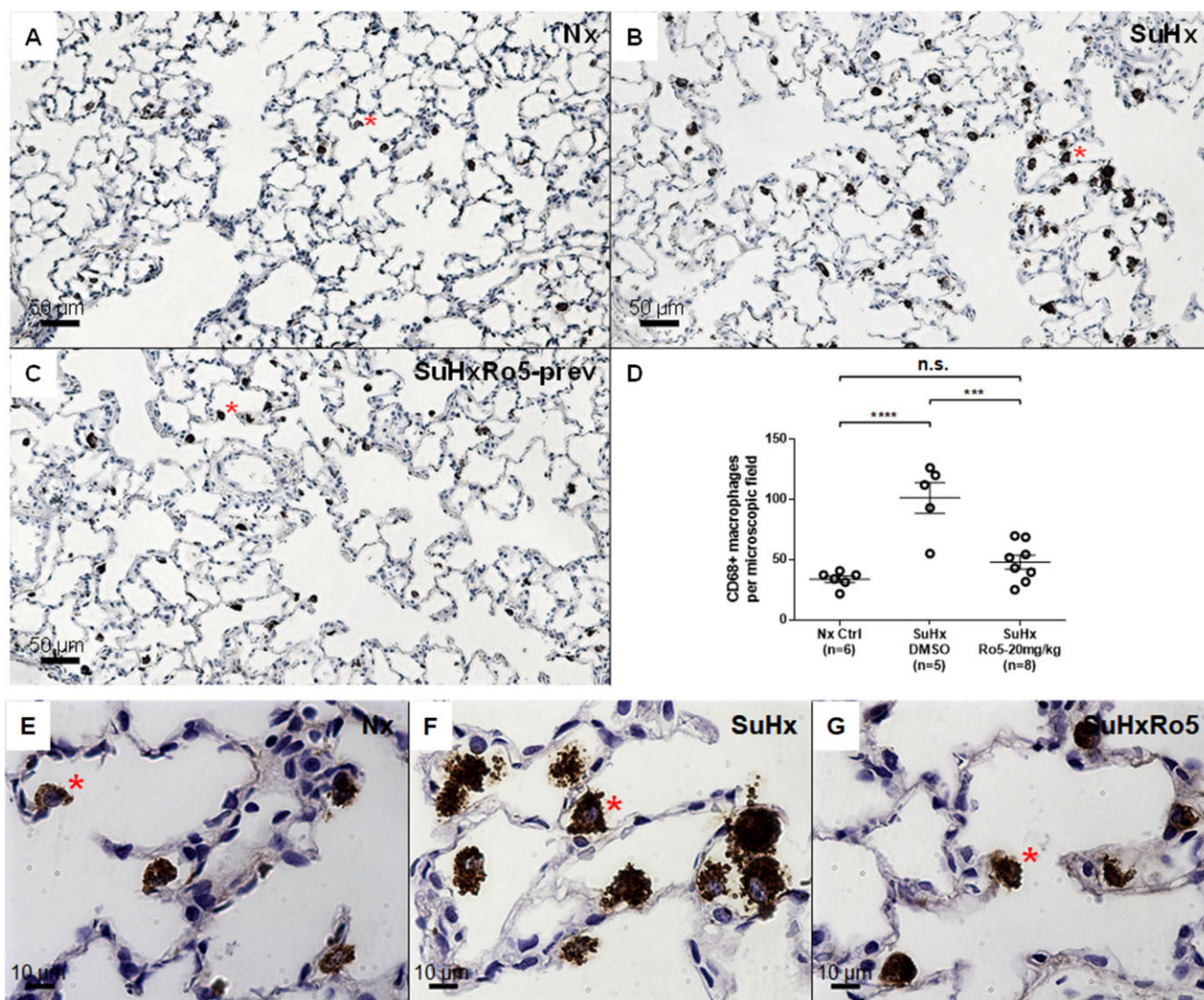


**Figure 2** Inhibition of RUNX1 *in vivo* reduces macrophage recruitment in the lung of SuHx-treated rats. (A–C) Representative microscopic images of 100× magnification show IHC staining in dark brown colour of CD68+ macrophages in the lung of Nx rats (A), vehicle DMSO-treated SuHx rats (B), and Ro5-treated SuHx rats (C). (D) Three representative images of 100× magnification of the staining were taken for each sample and the number of CD68+ macrophages in each image was manually counted. A summary of the numbers of CD68+ macrophages per microscopic field is shown. (E–G) Representative macrophages stained in dark brown colour for CD68, which are labelled with a red asterisk in (A–C), are shown in 600× magnification: (E) Nx Ctrl rats; (F) vehicle DMSO-treated SuHx rats; and (G) Ro5-treated SuHx rats. \*\*\* $P < 0.001$ , \*\*\*\* $P < 0.0001$ , n.s.: not significant, ordinary one-way ANOVA with multiple comparisons,  $n$  = number of animals in each experimental group.

## 2.4 Inducibly labelling of ECs/EPCs in adult VE-cadherin-CreERT2; ZsGreen mice and lineage tracing *in vivo* under SuHx conditions

All mice (summarized in [Supplementary material online, Table S1](#)) were maintained in pathogen-free conditions and all procedures were approved by the Lifespan IACUC. The inducible endothelial-specific VE-cadherin-CreERT2 mice<sup>20,21</sup> were obtained from Dr Iruela-Arispe (University of California, Los Angeles, CA), and genotyping for these mice was performed with the following primers: VE-cadherin common forward 5'-GCA GGC AGC TCA CAA AGG AAC AAT-3'; VE-cadherin reverse 5'-TGT CCT TGC TGA GTG ACA GTG GAA-3'; and

VE-cadherin Cre reverse 5'-ATC ACT CGT TGC ATC GAC CGG TAA-3'. The Rosa26-LSL-ZsGreen reporter mice [B6.Cg-Gt(ROSA)26Sor(tm6)(CAG-ZsGreen1)Hze/], JAX #007906] were purchased from the Jackson Laboratory (Bar Harbor, ME), and genotyping for these mice was performed according to the vendor's protocol. Male VE-cadherin-CreERT2 mice were crossbred with female Rosa26-LSL-ZsGreen reporter mice to generate VE-cadherin-CreERT2; ZsGreen mice (see [Supplementary material online, Figure S5A](#)). Adult double transgenic mice of 10–13 weeks of age with correct genotype were used for lineage tracing experiments. Briefly, the inducible double transgenic mice were each given 2 mg of tamoxifen (Tam) (MilliporeSigma) dissolved in 100  $\mu$ L of corn oil (MilliporeSigma) daily via intraperitoneal injection for 5 days followed by 1 week of incubation. Subsequent SuHx

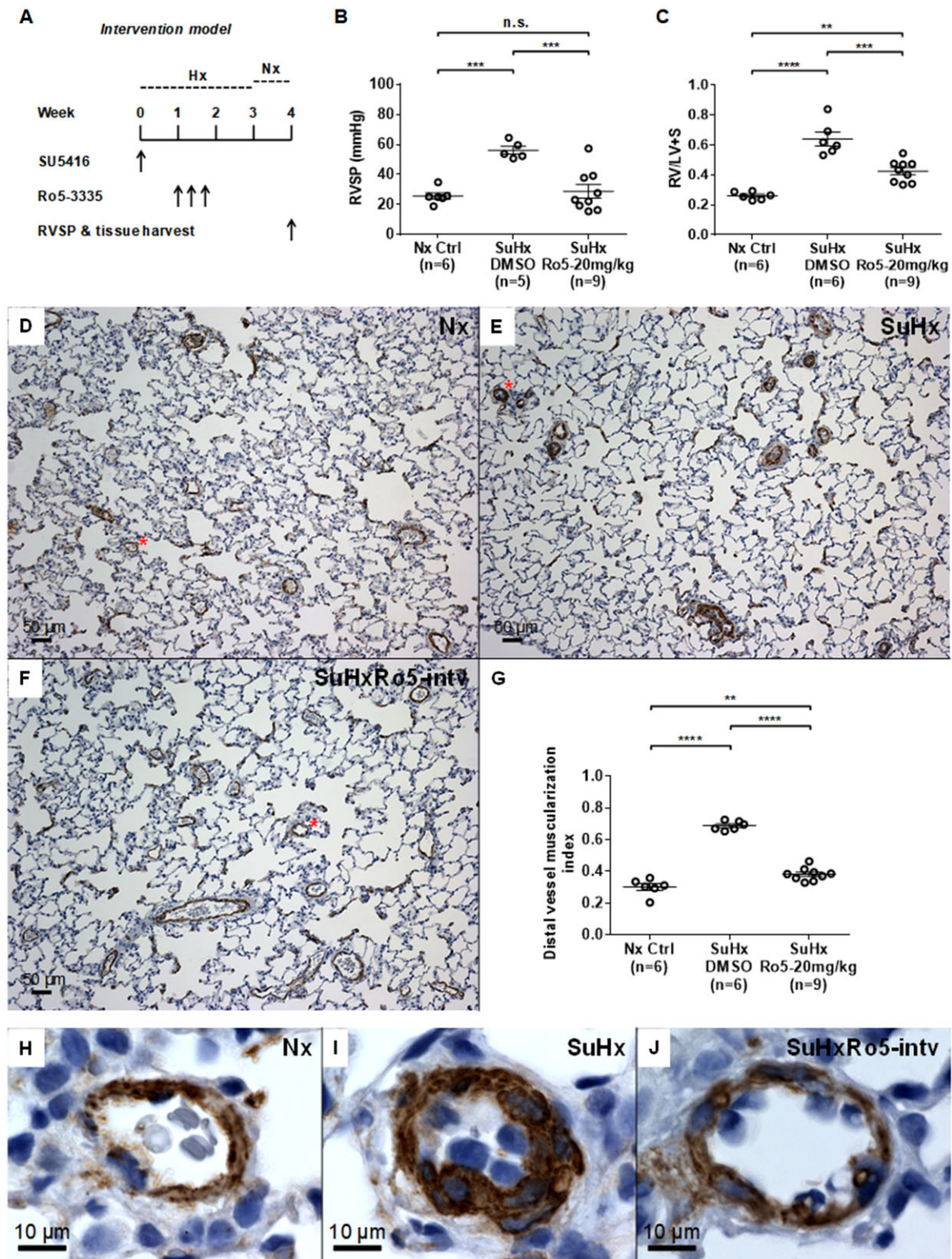


**Figure 3** Inhibition of RUNX1 *in vivo* blocks the progression of SuHx-PH in rats. (A) Experimental protocol for intervention of SuHx-PH in rats shows administration of the RUNX1 inhibitor Ro5-3335 every other day for three times 1 week after the beginning of SuHx treatment. (B and C) RVSP (B) and RV/LV + S ratio (C) were measured 1 week after removal from 3 weeks of Hx. (D–F) Representative microscopic images of 100× magnification show IHC staining in brown colour of  $\alpha$ -SMA in the blood vessels from lungs of Nx Ctrl rats (D), vehicle DMSO-treated SuHx rats (E) and Ro5-treated SuHx rats (F). (G) Muscularization of distal pulmonary vessels less than 50  $\mu$ m in diameter was assessed by calculating the muscularization index. (H–J) Representative small blood vessels stained in brown colour of  $\alpha$ -SMA, which are labelled with a red asterisk in (D–F), are shown in 600× magnification: (H) Nx Ctrl rats; (I) vehicle DMSO-treated SuHx rats; and (J) Ro5-treated SuHx rats. \*\* $P < 0.01$ , \*\*\* $P < 0.001$ , \*\*\*\* $P < 0.0001$ , n.s.: not significant, ordinary one-way ANOVA with multiple comparisons,  $n$  = number of animals in each experimental group.

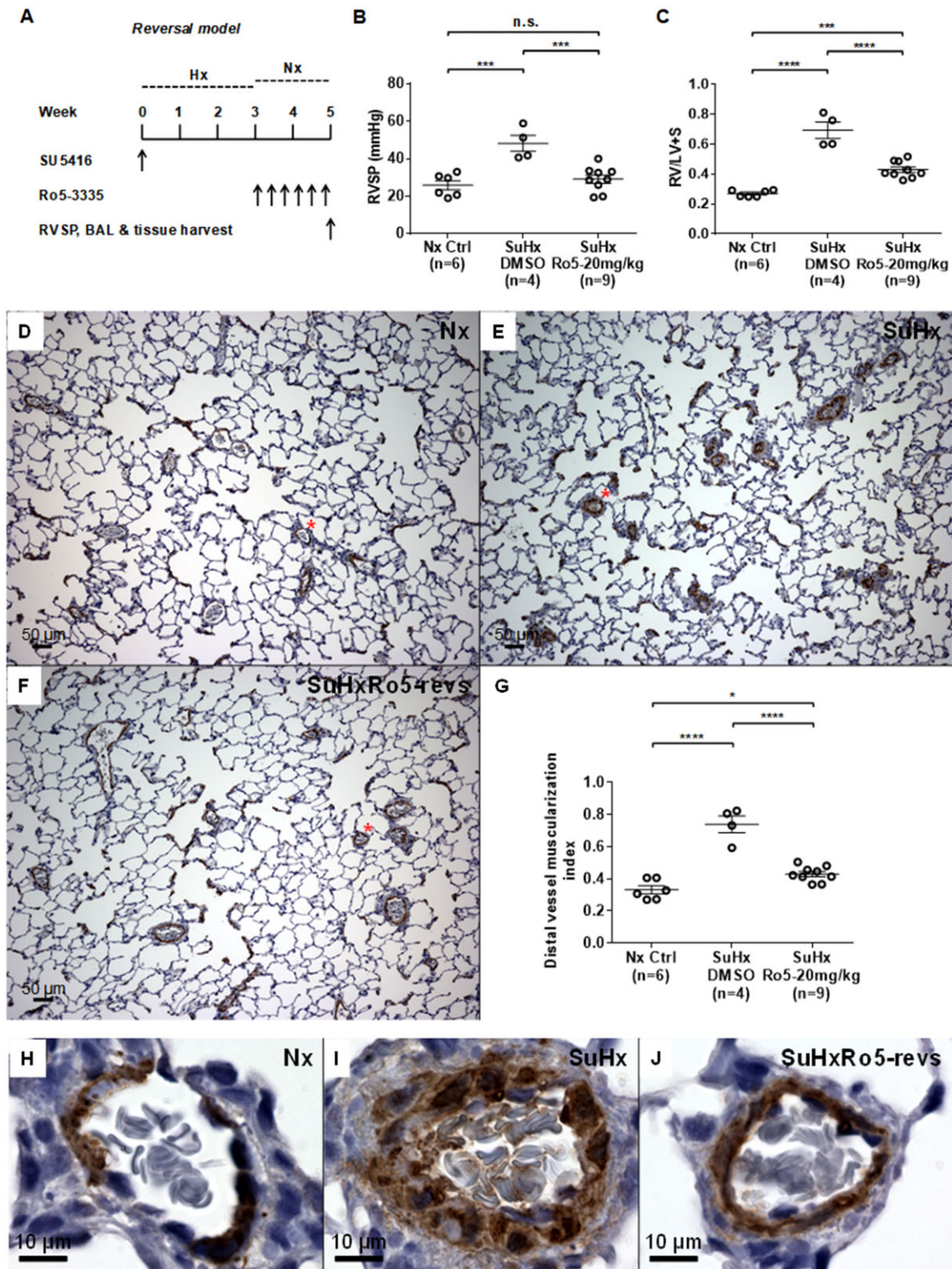


**Figure 4** Inhibition of RUNX1 *in vivo* reverses established SuHx-PH in rats. (A) Experimental protocol for reversal of SuHx-PH in rats shows administration of the RUNX1 inhibitor Ro5-3335 every other day for six times after the completion of SuHx treatment. (B and C) RVSP (B) and RV/LV + S ratio (C) were measured 2 weeks after removal from 3 weeks of Hx. (D–F) Representative microscopic images of 100 $\times$  magnification show IHC staining in brown colour of  $\alpha$ -SMA in the blood vessels from lungs of Nx Ctrl rats (D), vehicle DMSO-treated SuHx rats (E) and Ro5-treated SuHx rats (F). (G) Muscularization of distal pulmonary vessels less than 50  $\mu$ m in diameter was assessed by calculating the muscularization index. (H–J) Representative small blood vessels stained in brown colour of  $\alpha$ -SMA, which are labelled with a red asterisk in (D–F), are shown in 600 $\times$  magnification: (H) Nx Ctrl rats; (I) vehicle DMSO-treated SuHx rats; and (J) Ro5-treated SuHx rats. \* $P < 0.05$ , \*\*\* $P < 0.001$ , \*\*\*\* $P < 0.0001$ , n.s.: not significant, ordinary one-way ANOVA with multiple comparisons,  $n$  = number of animals in each experimental group.

treatment consisted of 3 weekly subcutaneous injections of the Sugen VEGF receptor 2 inhibitor SU5416 at 20 mg/kg in 100  $\mu$ L DMSO or vehicle alone. Concurrent with the SU5416 treatment, the double transgenic mice were exposed to Hx (8.5% O<sub>2</sub>) or normoxia (Nx) for 3 weeks, and 50  $\mu$ L of peripheral blood samples were collected weekly by retro-orbital bleeding from each mouse (see [Supplementary material online, Figure S5B](#)). For anaesthesia during retro-orbital blood sampling, the mice were anaesthetized via intraperitoneal injection with ketamine (100 mg/kg) and xylazine (10 mg/kg). For euthanasia, the mice were euthanized via CO<sub>2</sub> asphyxia followed by cervical dislocation. After red blood cell lysis, the rest of the cells in the blood samples were washed with PBS and stained with antibodies against mouse CD45 conjugated with Allophycocyanin (APC) (BioLegend, San Diego, CA). Flow cytometry analysis was performed on a 4-laser LSR II flow cytometer (BD Biosciences), and data were analysed with the FlowJo software.

## 2.5 Genetic deletion of *Runx1* in adult ECs/EPCs to prevent SuHx-PH in mice

We have previously used the constitutive VE-cadherin-Cre mice (JAX #006137) from the Jackson Laboratory and the inducible VE-cadherin-CreERT2 mice from Dr Iruela-Arispe's lab (UCLA) (see [Supplementary material online, Table S1](#)). However, in order to most efficiently delete the *Runx1* gene in adult ECs/EPCs, we have also purchased the Cdh5(PAC)-CreERT2 mouse developed by Dr Ralf Adams<sup>22</sup> (Taconic #13073, Taconic Biosciences, Rensselaer, NY). Upon Tam induction, this mouse line has a significantly better VE-cadherin promoter driven Cre-mediated recombination in ECs/EPCs than the UCLA mouse line (Personal communication, 2018 Gordon Research Conference on Endothelial Cells). We have also established the *Runx1*(flox/flox) mouse colony (JAX #008772, Jackson Laboratory, Bar Harbor, ME) in our lab. We then crossbred them to generate Cdh5-CreERT2; *Runx1*(fl/fl) mice ([Figure 5A](#)). Mice with correct genotype were each treated with 2 mg of Tam daily via intraperitoneal injection for 5 days followed by 1 week of incubation to delete *Runx1* gene in adult ECs/EPCs. Lung ECs from the mice treated with Tam were isolated via flow cytometry cell sorting,<sup>23</sup> and the loss of *Runx1* in ECs was verified per qRT-PCR with the following primers: forward 5'-CCT CCT TGA ACC ACT CCA CT-3', and reverse 5'-CTG GAT CTG CCT GGC ATC-3'. *GAPDH* expression was assessed per qRT-PCR as an internal reference for quantification with the following primers: forward 5'-AAA AGC AAC TCC CAC TCT TC-3' and reverse 5'-CCT GTT GCT GTA GCC GTA TT-3'. All PCR primers were synthesized by Integrated DNA Technologies (Coralville, IA). As a control experiment to test the endothelial specificity of *Runx1* deletion, we also evaluated *Runx1* gene expression in CD14<sup>+</sup> monocytes isolated from BM of these mice following Tam induction. An anti-mouse CD14 antibody conjugated with APC was purchased from BioLegend and BM CD14<sup>+</sup> cells were sorted on a BD Influx flow cytometry cell sorter (BD Biosciences). For SuHx-PH induction, similar to described above in [Supplementary material online, Figure S5B](#), Tam was given daily via intraperitoneal injection for 5 days followed by 1 week of incubation before the 3 weeks SuHx treatment of the Cdh5-CreERT2; *Runx1*(fl/fl) mice. Development of PH in mice was determined by measurement of right ventricular systolic pressure (RVSP) and right ventricular (RV) hypertrophy [assessed by the Fulton's index, i.e. RV to left ventricle + septum wet weight ratio (RV/LV + S)] as described in our previous study.<sup>13</sup>

## 2.6 Genetic deletion of *Runx1* in cells of myeloid lineage to prevent SuHx-PH in mice

LysM-Cre mice (JAX #004781) from the Jackson Laboratory allow for both specific and highly efficient Cre-mediated deletion of loxP-flanked target genes in myeloid cells: a deletion efficiency of 83–98% was determined in mature macrophages and near 100% in granulocytes.<sup>24,25</sup> We crossbred the LysM-Cre mice with the *Runx1*(flox/flox) mice to generate LysM-Cre; *Runx1*(fl/fl) mice ([Figure 6A](#)). The loss of *Runx1* in flow cytometry sorted BM-derived CD14<sup>+</sup> monocytes was verified per qRT-PCR as described above. Subsequent SuHx treatment consisted of three weekly subcutaneous injections of the Sugen VEGF receptor 2 inhibitor SU5416 at 20 mg/kg in 100  $\mu$ L DMSO. Concurrent with the SU5416 treatment, the transgenic mice were exposed to Hx (8.5% O<sub>2</sub>) for 3 weeks. Development of PH in mice was determined by measurement of RVSP and RV hypertrophy as described in our previous study.<sup>13</sup>

## 2.7 Macrophage polarization *in vitro*

Macrophage polarization *in vitro* was carried out as published previously,<sup>15</sup> which is also described in detail in [Supplementary material online](#).

## 2.8 Statistical analysis

Data are shown as the mean values  $\pm$  standard error of the mean. The significance of difference was calculated with unpaired two-tailed Student's *t*-test or one-way ANOVA when comparing more than two groups by using the GraphPad Prism programme (GraphPad Software, Inc., La Jolla, CA). *P*-values less than 0.05 were considered to be statistically significant.

# 3. Results

## 3.1 Inhibition of RUNX1 *in vivo* prevents the development of SuHx-PH in rats

Compared with Nx control rats, SuHx treatment caused severe PH in rats as evidenced by marked increases in RVSP, RV hypertrophy, and striking vascular remodelling in the lung.<sup>19</sup> In the disease prevention model of the present study ([Figure 1A](#)), vehicle-treated SuHx rats developed elevated RVSP compared with Nx control rats ([Figure 1B](#)). RVSP in rats given the RUNX1 inhibitor Ro5-3335 (SuHxRo5) at the beginning of SuHx treatment was significantly lower than SuHx rats given vehicle alone, and was no different than in Nx control rats ([Figure 1B](#)). SuHx treatment also caused significant RV hypertrophy compared with the Nx rats as indicated by an increase in the Fulton's index (RV/LV + S ratio) ([Figure 1C](#)). However, the Fulton's index was lower in rats treated with the RUNX1 inhibitor than in SuHx rats given vehicle alone ([Figure 1C](#)). Compared with the Nx control rats ([Figure 1D and H](#)), SuHx rats developed marked vascular remodelling as indicated by an increase in muscularization of peripheral pulmonary vessels ([Figure 1E and I](#)), which was significantly reduced in rats treated with the RUNX1 inhibitor ([Figure 1F and J](#)). The distal pulmonary vessel (i.e. pulmonary arteriole) muscularization indexes in the prevention model are summarized in [Figure 1G](#). Combined, these results suggest that inhibition of RUNX1 early on can effectively prevent the development of PH.

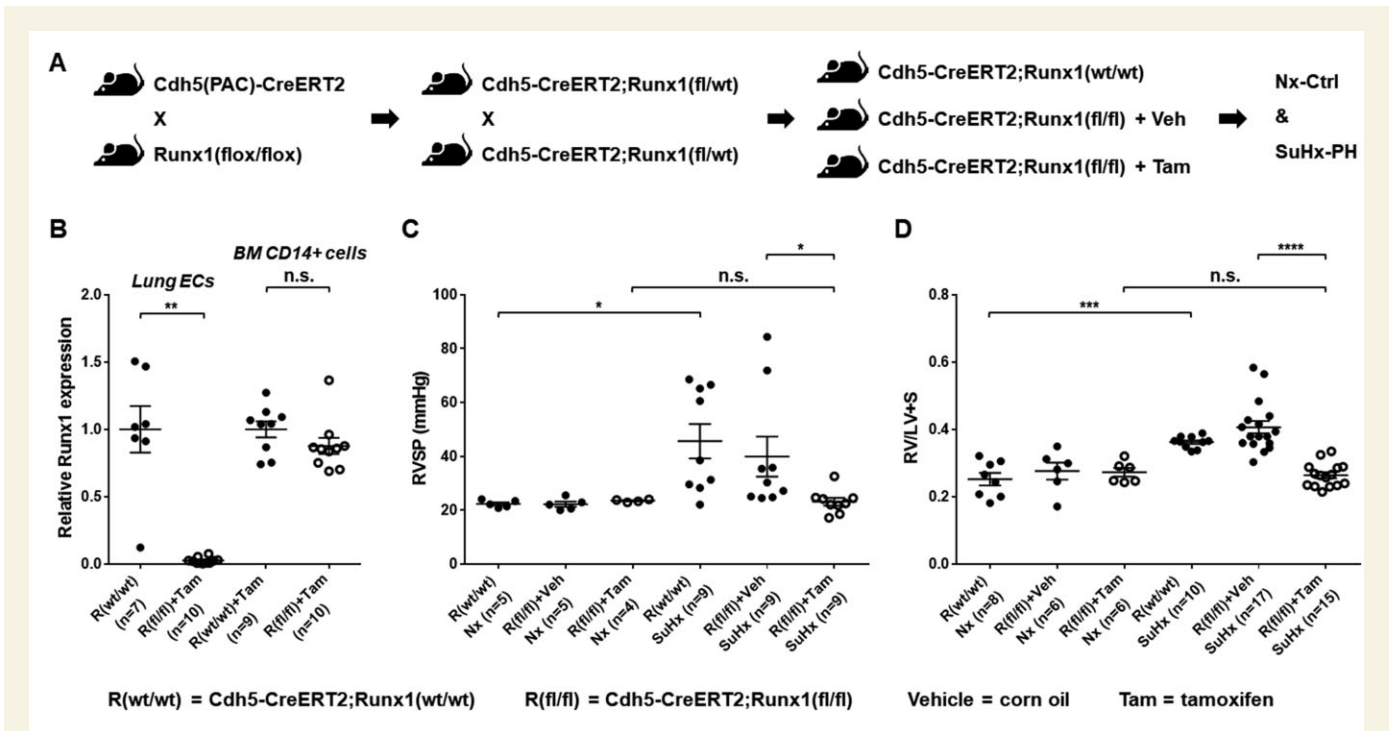


**Figure 5** Genetic deletion of *Runx1* in adult ECs/EPCs prevents SuHx-PH development in mice. (A) Experimental design to crossbreed Cdh5(PAC)-CreERT2 and Runx1(flox/flox) mice to generate Cdh5-CreERT2; Runx1(fl/fl) mice, which were then subjected to tamoxifen treatment followed by SuHx-PH induction. (B) In 10- to 13-week-old mice, the loss of *Runx1* in lung endothelial cells (ECs) upon Tam induction was verified per qRT-PCR. No changes in *Runx1* gene expression in BM-derived CD14<sup>+</sup> cells were found, demonstrating the endothelial specificity of *Runx1* deletion in these mice. (C and D) Under Nx conditions, Cdh5-CreERT2; Runx1(wt/wt) mice, Cdh5-CreERT2; Runx1(fl/fl) mice treated with corn oil, and Cdh5-CreERT2; Runx1(fl/fl) mice treated with Tam all exhibited normal RVSP (C) and RV/LV + S ratio (D). Under SuHx conditions, Cdh5-CreERT2; Runx1(wt/wt) mice and Cdh5-CreERT2; Runx1(fl/fl) mice treated with corn oil exhibited significantly elevated RVSP (C) and RV/LV + S ratio (D). When the Cdh5-CreERT2; Runx1(fl/fl) mice were treated with Tam and placed under SuHx conditions, they exhibited normal RVSP (C) and RV/LV + S ratio (D). \* $P < 0.05$ , \*\* $P < 0.01$ , \*\*\* $P < 0.001$ , \*\*\*\* $P < 0.0001$ , n.s.: not significant, unpaired two-tailed Student's *t*-test (B) and ordinary one-way ANOVA with multiple comparisons (C and D), *n* = number of animals in each experimental group.

### 3.2 Inhibition of RUNX1 *in vivo* reduces macrophage recruitment in the lung of SuHx-treated rats

In the prevention model, we quantified the macrophages in the lung following immunohistochemical staining of CD68, which is a pan-macrophage marker for rats.<sup>26</sup> Compared with the Nx rats (Figure 2A and E), the SuHx rats had significantly increased number of CD68<sup>+</sup> macrophages (stained brown), many of which morphologically appeared to have been in an activated state as suggested by their expanded sizes and the formation of membrane blebs (Figure 2B and F). Treatment with the RUNX1 inhibitor effectively prevented macrophage recruitment in the lungs of SuHx-treated rats (Figure 2C and G). The numbers of CD68<sup>+</sup> macrophages in the prevention model are summarized in Figure 2D. These results suggest that inhibition of RUNX1 *in vivo* at the onset of the process can significantly reduce macrophage recruitment in the lung during SuHx induction of PH.

### 3.3 Inhibition of RUNX1 *in vivo* blocks the progression of SuHx-PH in rats

In the disease intervention model of the current study (Figure 3A), SuHx treatment caused a significantly elevated RVSP in rats compared with Nx control rats (Figure 3B). However, when rats received the RUNX1

inhibitor Ro5-3335 1 week after the onset of SuHx induction of PH, their average RVSP was significantly lower than that of the SuHx rats treated only with the vehicle, and had no difference compared with the Nx control rats (Figure 3B). Compared with the Nx control rats, SuHx treatment led to a higher Fulton's index suggesting the development of RV hypertrophy (Figure 3C). However, compared with the vehicle-treated SuHx rats, the degree of RV hypertrophy was significantly diminished when rats were treated with the RUNX1 inhibitor (Figure 3C). Compared with the Nx control rats (Figure 3D and H), the SuHx rats developed marked vascular remodelling as indicated by the  $\alpha$ -SMA staining in brown colour (Figure 3E and I), which was significantly inhibited when the rats were treated with the RUNX1 inhibitor (Figure 3F and J). The distal pulmonary vessel (i.e. pulmonary arteriole) muscularization indexes in the intervention model are summarized in Figure 3G. Combined, these results suggest that inhibition of RUNX1 *in vivo* during disease development can effectively block the progression of SuHx-PH.

### 3.4 Inhibition of RUNX1 *in vivo* reverses established SuHx-PH in rats

In the reversal model, rats received extended RUNX1 inhibition after SuHx-induced PH had already established (Figure 4A). SuHx rats treated with vehicle alone developed elevated RVSP compared with Nx control rats (Figure 4B). Treatment with the RUNX1 inhibitor Ro5-3335



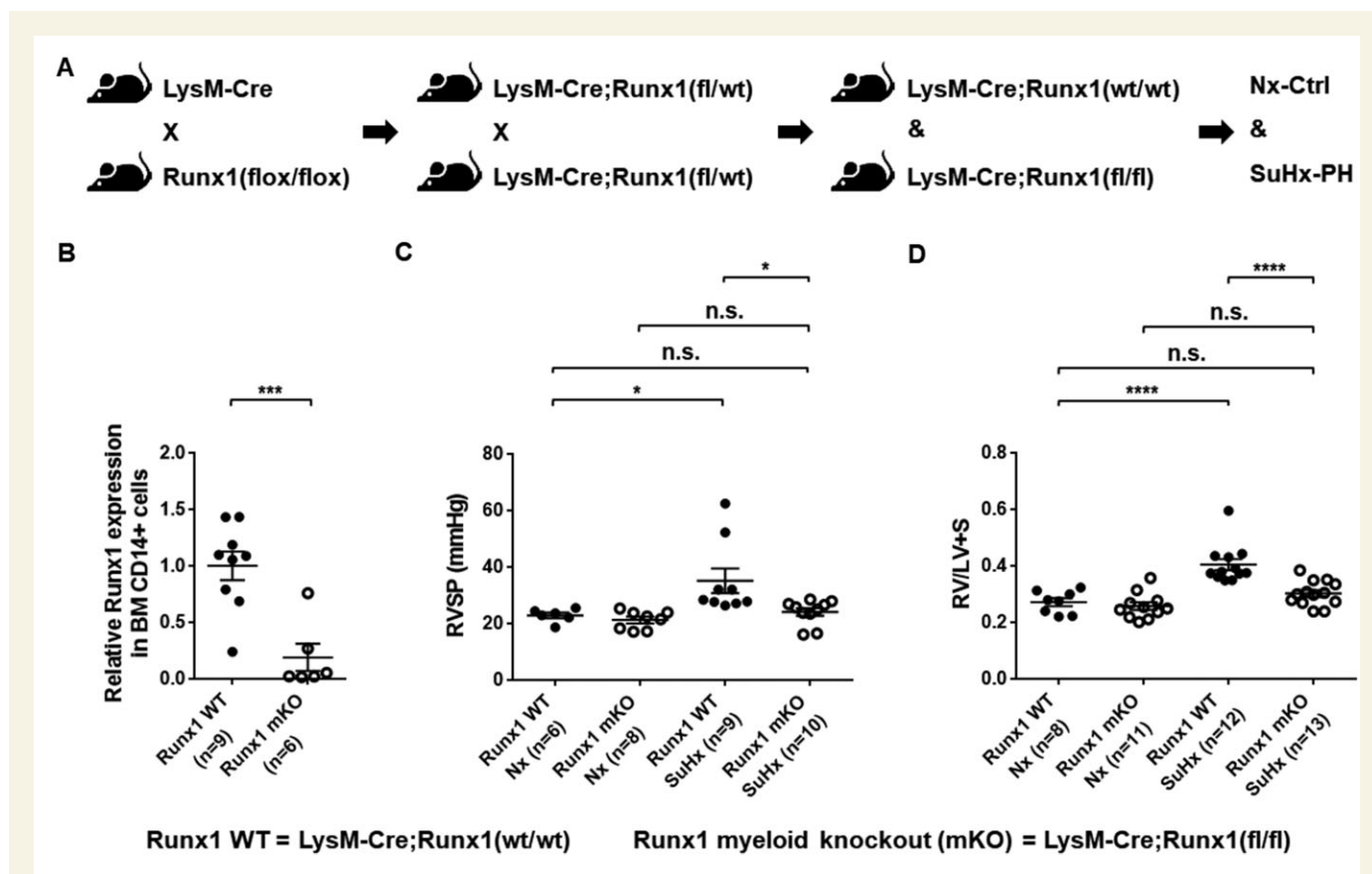


**Figure 6** Genetic deletion of *Runx1* in cells of myeloid lineage prevents SuHx-PH development in mice. (A) Experimental design to crossbreed LysM-Cre and *Runx1(flox/flox)* mice to generate LysM-Cre; *Runx1(fl/fl)* mice, which were then subjected to SuHx-PH induction. (B) In 10- to 13-week-old mice, the loss of *Runx1* in flow cytometry sorted BM-derived CD14<sup>+</sup> monocytes was verified per qRT-PCR. (C and D) Under Nx conditions, LysM-Cre; *Runx1(wt/wt)* mice and LysM-Cre; *Runx1(fl/fl)* mice exhibited normal RVSP (C) and RV/LV + S ratio (D). Under SuHx conditions, LysM-Cre; *Runx1(wt/wt)* mice developed elevated RVSP (C) and RV/LV + S ratio (D), whereas the LysM-Cre; *Runx1(fl/fl)* mice maintained normal RVSP (C) and RV/LV + S ratio (D). \* $P < 0.05$ , \*\*\* $P < 0.001$ , \*\*\*\* $P < 0.0001$ , n.s.: not significant, unpaired two-tailed Student's *t*-test (B) and ordinary one-way ANOVA with multiple comparisons (C and D), *n* = number of animals in each experimental group.

significantly reduced RVSP in SuHxRo5 rats when compared with the vehicle-treated SuHx rats, and reversed RVSP to the level comparable to that of the Nx control rats (Figure 4B). SuHx induction of PH resulted in prominent RV hypertrophy in the SuHx rats compared with the Nx control rats as indicated by the Fulton's index (Figure 4C). However, the severity of RV hypertrophy was significantly attenuated in rats that were given the RUNX1 inhibitor when compared with the vehicle-treated SuHx rats (Figure 4C). Compared with the Nx control rats (Figure 4D and H), the SuHx rats developed marked vascular remodelling as indicated by the  $\alpha$ -SMA staining in brown colour (Figure 4E and I), which was significantly reversed when the rats were treated with the RUNX1 inhibitor (Figure 4F and J). The distal pulmonary vessel (i.e. pulmonary arteriole) muscularization indexes in the reversal model are summarized in Figure 4G. In addition, we also demonstrated that there were no effects of Ro5-3335 on RVSP and RV/LV + S ratio in normal rats after a 2-week long treatment (see Supplementary material online, Figure S1A–C). Combined, these results suggest that inhibition of RUNX1 *in vivo* after the completion of SuHx induction of PH can effectively reverse established disease.

### 3.5 Inhibition of RUNX1 *in vivo* depletes alveolar macrophages in rats

Alveolar macrophages in the BAL consist of resident alveolar macrophages derived from yolk sac precursors of foetal monocytes and BM monocyte-derived macrophages following inflammatory insults.<sup>27</sup> In the reversal model, rats received extended RUNX1 inhibition after SuHx-induced PH had already established. Flow cytometry analysis showed that in Nx control rats CD68<sup>+</sup> macrophages accounted for an average  $75.3 \pm 2.0\%$ , but in Nx rats treated with the RUNX1 inhibitor, CD68<sup>+</sup> macrophages were almost completely depleted and accounted for an average  $1.6 \pm 0.3\%$  of the cellular content of the BAL (see Supplementary material online, Figure S1D). In SuHx rats, CD68<sup>+</sup> macrophages accounted for an average  $64.9 \pm 6.5\%$  of the cellular content of the BAL, which is comparable with that in the Nx rats. SuHx rats that received RUNX1 inhibition in our reversal protocol had significantly fewer CD68<sup>+</sup> macrophages ( $56.4 \pm 8.5\%$ ) than that of the Nx rats, but the alveolar macrophage number was not significantly lower than that of the SuHx-PH rats (see Supplementary material online, Figure S1D).

### 3.6 Inhibition of RUNX1 *in vivo* has no effect on pulmonary arteriole density in rats

We counted all distal pulmonary vessels less than 50  $\mu\text{m}$  in diameter that were stained  $\alpha\text{-SMA}^+$  in the above three study protocols and then compared the numbers between SuHx treated rats with and without RUNX1 inhibition. Our results suggest that inhibition of RUNX1 *in vivo* has no effect on pulmonary arteriole density among SuHx treated rats (see [Supplementary material online, Figure S2](#)).

### 3.7 No immediate vasodilatory improvement of SuHx-PH in mice by the RUNX1 inhibitor Ro5-3335

To investigate if the RUNX1 inhibitor Ro5-3335 may alleviate SuHx-PH in rodent models through pulmonary vasodilatory properties, we injected C57BL/6j mice with 20 mg/kg Ro5-3335 following 3 weeks of SuHx-PH induction and assessed RVSP and RV hypertrophy at 1 h or 3 h after Ro5-3335 injection (see [Supplementary material online, Figure S3A](#)). As shown in [Supplementary material online, Figure S3B and C](#), no reductions of RVSP or RV hypertrophy were seen at these two time points following Ro5-3335 injection. These results, which show no immediate vasodilatory improvement of SuHx-PH in mice by the RUNX1 inhibitor Ro5-3335, suggest that Ro5-3335 does not act as a vessel dilator.

### 3.8 Inducibly labelling of adult ECs/EPCs in mice and lineage tracing demonstrates haematopoietic transformation of ECs *in vivo*

We generated the VE-cadherin-CreERT2; ZsGreen double transgenic mice (see [Supplementary material online, Figure S5A and Table S1](#)), which were treated with 2 mg of Tam daily for 5 days followed by 1 week of incubation before SuHx-PH induction (see [Supplementary material online, Figure S5B](#)). Our results of adult lung endothelium labelling upon Tam induction in these mice are demonstrated and quantified in [Supplementary material online, Figure S4A–G](#), which suggested an age-dependent labelling efficiency similar with published results.<sup>20,21</sup> In  $\text{Cre}^{+/-}\text{ZsG}^{+/-}$  mice, there is an extremely low level (e.g. 0.032%) of background of  $\text{CD45}^+\text{ZsG}^+$  cells upon Tam induction, compared with  $\text{Cre}^{+/-}\text{ZsG}^{+/-}$  mice without Tam induction or  $\text{Cre}^{+/-}\text{ZsG}^{-/-}$  mice with Tam induction (see [Supplementary material online, Figure S5C](#)). However, when a Tam induced  $\text{Cre}^{+/-}\text{ZsG}^{+/-}$  mouse (#917) was treated with SuHx, the  $\text{CD45}^+\text{ZsG}^+$  population in the PB of this mouse increased greater than 10-fold from the initial 0.074% at W0 to 0.32% at W1 and to 0.80% at W2 before returning to the background level at W3 (see [Supplementary material online, Figure S5D](#)). Another Tam-induced  $\text{Cre}^{+/-}\text{ZsG}^{+/-}$  mouse (#977) also produced a distinct  $\text{CD45}^+\text{ZsG}^+$  population (0.2%) at W1 compared with the initial 0% background (see [Supplementary material online, Figure S5D](#)). The generation of  $\text{CD45}^+\text{ZsG}^+$  new blood cells by ZsG-labelled adult endothelium in the VE-cadherin-CreERT2; ZsGreen double transgenic mice is quantitatively summarized in [Supplementary material online, Figure S6A](#). The significant difference in  $\text{CD45}^+$  cells that express ZsG before (W0) and after SuHx treatment (W1) in these mice would have to derive from ECs/EPCs in adulthood. The exhaustion of ZsG-labelled progenitor cells may be the reason for the disappearance of  $\text{CD45}^+\text{ZsG}^+$  cells at W3. The time course of expression for  $\text{CD45}^+\text{ZsG}^+$  cells in the Tam-inducible model over 3 weeks is similar to that in the constitutive model.<sup>13</sup> In our

first control experiment, Tam-induced  $\text{Cre}^{+/-}\text{ZsG}^{+/-}$  mice were placed in Nx instead of SuHx for 3 weeks, and there was no development of a  $\text{CD45}^+\text{ZsG}^+$  population in the PB of these mice (see [Supplementary material online, Figures S5E and S6B](#)). In our second control experiment,  $\text{Cre}^{+/-}\text{ZsG}^{+/-}$  mice were injected with vehicle corn oil without Tam followed by SuHx induction of PH, and there were no  $\text{CD45}^+\text{ZsG}^+$  cells in the PB of these mice throughout the 3 weeks of SuHx treatment (see [Supplementary material online, Figures S5F and S6C](#)). More importantly, we demonstrated that the emergence of  $\text{CD45}^+\text{ZsG}^+$  cells is RUNX1-dependent, as the RUNX1 inhibitor Ro5-3335 blocked the development of any such cells (see [Supplementary material online, Figure S6D and E](#)). This RUNX1-dependent transformation is reminiscent of that in the constitutive model which we reported earlier.<sup>13</sup> Combined, our lineage tracing experiments, in both constitutive and inducible mouse models, suggest that under pathological conditions, such as Hx or induction of PH, haematopoietic transformation of adult endothelium may occur in a RUNX1-dependent manner.

### 3.9 Genetic deletion of *Runx1* in adult ECs/EPCs prevents SuHx-PH development in mice

In order to conditionally delete *Runx1* gene in adult ECs/EPCs, we crossbred *Cdh5*(PAC)-CreERT2 and *Runx1*(flox/flox) mice to generate the *Cdh5*-CreERT2; *Runx1*(fl/fl) mice ([Figure 5A](#) and [Supplementary material online, Table S1](#)). At 10–13 weeks of age, these inducible double transgenic mice were each treated with 2 mg of Tam daily for 5 days followed by 1 week of incubation before SuHx-PH induction ([Figure 5A](#)). The loss of *Runx1* in mouse lung ECs upon Tam induction was verified per qRT-PCR ([Figure 5B](#)). In a control experiment to demonstrate the endothelial specificity of *Runx1* deletion in the *Cdh5*-CreERT2; *Runx1*(fl/fl) mice, we flow-sorted  $\text{CD14}^+$  monocytes from BM of these mice following tam induction. In comparison with controls, no changes of *Runx1* gene expression were found in the BM-derived  $\text{CD14}^+$  cells, indicating that endothelial deletion of *Runx1* did not affect *Runx1* expression in myeloid cells in this mouse model ([Figure 5B](#)). Under Nx conditions, *Cdh5*-CreERT2; *Runx1*(wt/wt) mice, *Cdh5*-CreERT2; *Runx1*(fl/fl) mice treated with corn oil, and *Cdh5*-CreERT2; *Runx1*(fl/fl) mice treated with Tam all exhibited normal RVSP and RV/LV + S ratio ([Figure 5C and D](#)). Under SuHx conditions, *Cdh5*-CreERT2; *Runx1*(wt/wt) mice and *Cdh5*-CreERT2; *Runx1*(fl/fl) mice treated with corn oil exhibited significantly elevated RVSP and RV/LV + S ratio ([Figure 5C and D](#)). However, when the *Cdh5*-CreERT2; *Runx1*(fl/fl) mice were treated with Tam and placed under SuHx conditions, they exhibited normal RVSP and RV/LV + S ratio, which were significantly less than those of the *Cdh5*-CreERT2; *Runx1*(fl/fl) mice treated with corn oil and placed under SuHx conditions, and were comparable with those values of the *Cdh5*-CreERT2; *Runx1*(fl/fl) mice treated with Tam but placed under Nx conditions ([Figure 5C and D](#)). These results suggest that genetic deletion of *Runx1* in adult ECs/EPCs prevents SuHx-PH development in mice.

### 3.10 Genetic deletion of *Runx1* in cells of myeloid lineage prevents SuHx-PH development in mice

We crossbred *LysM*-Cre and *Runx1*(flox/flox) mice to generate the *LysM*-Cre; *Runx1*(fl/fl) mice ([Figure 6A](#) and [Supplementary material online, Table S1](#)). In 10- to 13-week-old mice, the loss of *Runx1* in flow cytometry sorted BM-derived  $\text{CD14}^+$  monocytes was verified per qRT-PCR ([Figure 6B](#)). Under Nx conditions, *LysM*-Cre; *Runx1*(wt/wt) mice

and LysM-Cre; Runx1(fl/fl) mice exhibited normal RVSP and RV/LV + S ratio (Figure 6C and D). Under SuHx conditions, LysM-Cre; Runx1(wt/wt) mice developed elevated RVSP and RV/LV + S ratio. However, under SuHx conditions, the LysM-Cre; Runx1(fl/fl) mice maintained normal RVSP and RV/LV + S ratio, which were significantly less than those of the LysM-Cre; Runx1(wt/wt) mice under SuHx conditions, and were comparable with those values of the LysM-Cre; Runx1(fl/fl) mice kept in Nx (Figure 6C and D). These results suggest that genetic deletion of *Runx1* in cells of myeloid lineage prevents SuHx-PH development in mice.

### 3.11 Inhibition of RUNX1 dampens macrophage activation *in vitro*

We used different sets of cell surface markers (CD14+CD80+ and CD68+CD80+) to quantify M1-polarized activation of human bone marrow mononuclear cells (BMMNCs). Compared with untreated cells, LPS and IFN- $\gamma$  treatment drastically increased the expression of CD14, CD68, and CD80 in BMMNCs. Co-incubation of BMMNCs with the RUNX1 inhibitor Ro5-3335, but not with vehicle alone, decreased M1-polarized activation in a dose-dependent manner (see [Supplementary material online, Figure S7A and B](#)). We also used different sets of cell surface markers (CD163+CD206+ and CD11b+CD206+) to indicate M2-polarized activation of BMMNCs. Compared with untreated cells, IL-4 and IL-13 treatment increased the expression of CD11b, CD163, and CD206 in BMMNCs. Co-incubation of BMMNCs with the RUNX1 inhibitor Ro5-3335 had little effect on M2-polarized activation, although a non-significant trend towards reduced M2 macrophages was seen at the highest dose tested (see [Supplementary material online, Figure S7C and D](#)). Similarly, compared with untreated cells, M1-polarized activation of human THP1 cells drastically increased the expression of CD14, CD80, and HLA-DR. Co-incubation of THP1 cells with Ro5-3335, but not with vehicle alone, decreased M1-polarized activation in a dose-dependent manner (see [Supplementary material online, Figure S7E and F](#)). Combined, these results indicate that inhibition of RUNX1 can effectively dampen overall activation of macrophages.

## 4. Discussion

Perivascular infiltration by macrophages is well described in PAH and increasingly recognized as a major pathogenic component of pulmonary vascular remodelling.<sup>6,28–33</sup> Several studies have focused on the role of perivascular macrophages infiltrating pulmonary arterioles. CD68+ macrophages are prominent in advanced obliterative plexiform lesions observed in experimental and clinical PH,<sup>33</sup> and Florentin *et al.*<sup>34</sup> have recently reported that inflammatory macrophage expansion in PH depends upon mobilization of blood-borne monocytes. Blocking CD68+ macrophage-derived leukotriene B4 prevents endothelial injury and reverses PH in animal models of the disease.<sup>35</sup> However, a recently completed multi-centre prospective clinical trial of the leukotriene B4 inhibitor (Ubenimex) was not successful,<sup>36</sup> nor was another trial of the IL-1 $\beta$  receptor blocker anakinra.<sup>37</sup> These failures suggest that blocking one or more pro-inflammatory mediators will not be sufficient to impede PAH development. Hence, our goal of the current study was to reverse established PH by: (i) reducing the overall macrophage production through blocking RUNX1-dependent myeloid-skewed haematopoiesis; and (ii) inhibiting RUNX1-dependent macrophage recruitment and activation.

In the present study, we used conditional labelling of adult endothelium and lineage tracing to demonstrate that during the induction of PH, a small proportion of adult ECs/EPCs undergo haematopoietic transformation to yield cells of myeloid lineage and that this phenomenon is mediated by RUNX1. Inhibition of RUNX1 was effective at preventing such transformation, reducing macrophage recruitment in the lung and the classical pro-inflammatory activation. Furthermore, tissue-specific deletion of *Runx1* gene either in adult endothelium or in cells of myeloid lineage prevented the mice from developing SuHx-PH, suggesting that RUNX1 is required for the development of PH. Finally, in the rat model of SuHx-PH, administration of a RUNX1 inhibitor markedly attenuated RVSP, RV hypertrophy, and vascular remodelling in three separate protocols demonstrating that this approach was effective at preventing the disease, halting its progression and reversing established PH. Our additional experiments indicate that the RUNX1 inhibitor Ro5-3335 does not act as a vessel dilator in the short term. Combined, these findings extend our previously published observations of RUNX1 inhibition in murine models of PH and suggest that targeting RUNX1 may be an effective approach to treating PAH.

The importance of RUNX1-mediated haematopoietic transformation of ECs/EPCs in PH has been questioned due to the small number of myeloid cells that can be traced to endothelial lineage and to previous studies suggesting this transition does not occur in adult animals.<sup>38</sup> In our recent studies, we bred VE-cadherin-Cre; ZsGreen mice, and subjected these constitutive transgenic mice to SuHx induction of PH.<sup>13</sup> However, a small number of the haemangioblasts are known to have VE-cadherin promoter activity during early development of the embryo,<sup>39</sup> which may have resulted in labelling of some haematopoietic cells with ZsG, and made it difficult to distinguish *de novo* CD45+ cells that derived from the endothelium in adulthood. To eliminate this background in lineage tracing, we acquired the inducible VE-cadherin-CreERT2 mice. These mice have no constitutive expression of ZsG in embryonic haemangioblasts meaning that the generation of CD45+ZsG+ new blood cells in the VE-cadherin-CreERT2; ZsGreen double transgenic mice would have to derive from ECs/EPCs in adulthood. Importantly, CD45+ZsG+ were nearly undetectable in adult control mice, but increased approximately 10-fold within 2 weeks of starting SuHx and this increase was completely blocked by inhibition of RUNX1. Nonetheless, the number of myeloid cells that could be traced to endothelial lineage is most likely limited by the labelling efficiency of the inducible VE-cadherin-CreERT2; ZsGreen double transgenic mice used in the experiments. Our ability to characterize CD45+ZsG+ cells was very much limited due to the minuscule output of these cells after the inducible VE-cadherin-CreERT2; ZsGreen mice were treated with Tam and placed under SuHx conditions. Several studies suggest that the haemogenic endothelium is not as transient in nature as previously thought and may exist beyond the embryonic period as an untapped haematopoietic reservoir.<sup>40–42</sup> Our lineage tracing experiments, in both constitutive<sup>13</sup> and inducible mouse models in this study, suggest that under pathological conditions, haematopoietic transformation of ECs/EPCs may reactivate and contribute to adult haematopoiesis in a RUNX1-dependent manner.

Since homozygous *Runx1* knockout mice exhibit an embryonic lethal phenotype,<sup>12</sup> additional experiments with genetic deletion of *Runx1* in adult endothelium or in cells of myeloid lineage were performed in this study after the more superior Cdh5(PAC)-CreERT2 mouse developed by Dr Ralf Adams<sup>22</sup> became available to our lab. Importantly, our control experiments testing *Runx1* gene expression in the BM-derived CD14+ monocytes of Tam-induced Cdh5-CreERT2; Runx1(fl/fl) mice indicate that endothelial deletion of *Runx1* did not affect *Runx1* expression in

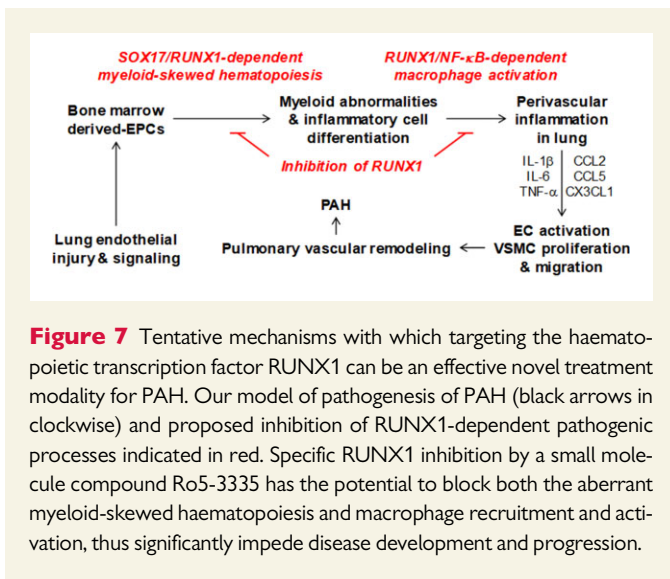


**Figure 7** Tentative mechanisms with which targeting the haematopoietic transcription factor RUNX1 can be an effective novel treatment modality for PAH. Our model of pathogenesis of PAH (black arrows in clockwise) and proposed inhibition of RUNX1-dependent pathogenic processes indicated in red. Specific RUNX1 inhibition by a small molecule compound Ro5-3335 has the potential to block both the aberrant myeloid-skewed haematopoiesis and macrophage recruitment and activation, thus significantly impede disease development and progression.

myeloid cells in this mouse model. A causative role for RUNX1 in PH is then strongly supported by the demonstration that tissue-specific knockout of *Runx1* in adult ECs/EPCs or in cells of myeloid lineage prevents SuHx-PH development in mice, and that inhibition of RUNX1 is sufficient to both prevent and reverse PH in mice and rat models of PH. Thus, the ability of RUNX1 to induce myeloid cell production through haematopoietic transformation of ECs/EPCs and to promote pro-inflammatory activation of monocytes/macrophages underscores its importance in the pathogenesis of PAH. Recently, several large scale patient studies utilizing whole genome sequencing in cohorts from Europe, the USA, and Japan have independently identified mutations in the *Sox17* enhancer region associated with PAH.<sup>43–47</sup> However, the mechanisms with which *Sox17* mutations lead to PAH is not understood. Notably, SOX17 can directly bind *Runx1* gene to repress haematopoietic cell fate during embryonic EHT,<sup>48</sup> and small perturbations in SOX17 levels are accompanied by concomitantly increased levels of RUNX1 driving haemogenic endothelium towards a haematopoietic fate.<sup>49</sup> Importantly, SOX17 was found to function as a switch that directs cell fate of CD34+ progenitors towards an endothelial vs. haematopoietic lineage.<sup>50,51</sup> Thus, it is possible that loss of repression of *Runx1* by SOX17 in ECs/EPCs facilitates myeloid-skewed haematopoietic transformation serving as the origin of inflammatory cells seen in PAH.

As a master-regulator transcription factor implicated in diverse signaling pathways and cellular mechanisms during normal development and disease, RUNX1 has recently also been proposed as a therapeutic target for cardiovascular disease.<sup>52</sup> McCarroll et al.<sup>53</sup> conducted a study using mice with an inducible cardiomyocyte-specific *Runx1* deficiency, and provided evidence that *Runx1* deficiency protects against adverse cardiac remodelling after myocardial infarction. This finding was later corroborated by other investigators as well.<sup>54,55</sup> Hence, novel therapies targeting RUNX1 may be efficacious by impacting on multiple downstream signaling pathways to mitigate adverse cardiac remodelling. Although transcription factors were thought as unlikely and challenging druggable targets in the past, transcription factor drivers of cancer have been directly targeted using small molecule inhibitors.<sup>56</sup> The compound Ro5-3335 and its analog Ro24-7429 were initially developed as anti-HIV drugs that block HIV gene expression by inhibiting Tat-mediated transactivation.<sup>57–59</sup> In 2012, Cunningham et al.<sup>18</sup> first reported that Ro5-3335 was able to directly interact with RUNX1 and its heterodimeric partner

CBFβ, repress RUNX1/CBFβ-dependent transactivation in reporter assays, and repress RUNX1-dependent haematopoiesis in zebrafish embryos. The investigators concluded that Ro5-3335 interacts with both RUNX1 and CBFβ, with stronger affinity for the former. However, Ro5-3335 does not disrupt RUNX1–CBFβ interaction completely, but changes the conformation of their complex or increases the distance between RUNX1 and CBFβ in the complex.<sup>18</sup> Ro5-3335 was subsequently used to inhibit RUNX1 in a variety of disease processes including in retinal angiogenesis<sup>60</sup> and acute myeloid leukaemia,<sup>61</sup> and to suppress macrophage-induced inflammation in septic shock.<sup>16</sup> Studies on pharmacokinetics and pharmacodynamics of Ro5-3335 have been conducted, and long-term administration of the compound is well-tolerated in mice.<sup>18</sup> In another series of studies, Illendula et al.<sup>62</sup> synthesized a library of analogs of compound AI-4-57 and characterized their activity as small molecule inhibitors of RUNX–CBFβ binding. The compound AI-4-57 was initially discovered to bind to the CBFβ portion of the CBFβ–SMMHC fusion protein and inhibits its binding to the Runt domain of RUNX proteins.<sup>63</sup> AI-4-57 and its derivatives may also be tested as candidates for RUNX1 inhibition in SuHx-PH rats in future studies. In summary, by blocking RUNX1-dependent myeloid-skewed haematopoiesis and macrophage recruitment and activation (Figure 7), inhibition of RUNX1 prevents and reverses PH in the SuHx-PH model in rats. It may be possible to use RUNX1 inhibitors to evaluate the role of RUNX1-dependent aberrant haematopoiesis and macrophage activation in patients with PAH. Thus, targeting RUNX1 may be a novel therapeutic approach in the treatment of PAH.

## Supplementary material

Supplementary material is available at *Cardiovascular Research* online.

## Authors' contributions

E.-M.J. and M.P.: Substantial contributions to study conception and design, analysis and interpretation of data, drafting and revision and final approval of manuscript, and agreement to be accountable for all aspects of the work. E.-Y.S., K.Q.W., M.D.T., S.W., and M.S.D.: Contributions to study design, acquisition, analysis, and interpretation of data, revision, and final approval of manuscript. P.M.D., A.M.R., C.E.V., P.J.Q., and J.R.K.: Contributions to interpretation of data and revision and final approval of manuscript. O.D.L.: Substantial contributions to study conception and design, data acquisition, analysis and interpretation of data, revision and final approval of manuscript, and agreement to be accountable for all aspects of the work.

## Data availability

The data that support the findings of this study are available from the corresponding author upon reasonable request.

## Acknowledgements

We wish to thank the Flow Cytometry Core of the COBRE Center for Stem Cells and Aging. We also thank Ginny Hovanessian for microscope imaging and Dongfang Yang for immunohistochemical staining.

**Conflict of interest:** none declared.

## Funding

This work was supported in part by grants from the National Institutes of Health P20 GM119943 (O.D.L. and P.J.Q.), P20 GM103652 (O.D.L.), R01 HL141268 (C.E.V.), and T32 HL116249 (E.-Y.S., O.D.L., and P.J.Q.), by the American Heart Association Transformational Project Award 18TPA34110329 (O.D.L.), the Rhode Island Foundation Medical Research Fund Nr. 5219\_20200595 (E.-M.J. and O.D.L.), and an Academic Assessment Research Award from the Brown Physicians, Inc. (O.D.L.).

## References

- Farber HW, Loscalzo J. Pulmonary arterial hypertension. *N Engl J Med* 2004;**351**:1655–1665.
- Simonneau G, Galie N, Rubin LJ, Langleben D, Seeger W, Domenighetti G, Gibbs S, Lebec D, Speich R, Beghetti M, Rich S, Fishman A. Clinical classification of pulmonary hypertension. *J Am Coll Cardiol* 2004;**43**:55–125.
- Simonneau G, Gatzoulis MA, Adatia I, Celermajer D, Denton C, Ghofrani A, Gomez Sanchez MA, Krishna Kumar R, Landzberg M, Machado RF, Olschewski H, Robbins IM, Souza R. Updated clinical classification of pulmonary hypertension. *J Am Coll Cardiol* 2013;**62**:D34–D41.
- McLaughlin VV, Shah SJ, Souza R, Humbert M. Management of pulmonary arterial hypertension. *J Am Coll Cardiol* 2015;**65**:1976–1997.
- Ventetuolo CE, Klinger JR. WHO Group 1 pulmonary arterial hypertension: current and investigative therapies. *Prog Cardiovasc Dis* 2012;**55**:89–103.
- Rabinovitch M, Guignabert C, Humbert M, Nicolls MR. Inflammation and immunity in the pathogenesis of pulmonary arterial hypertension. *Circ Res* 2014;**115**:165–175.
- Nicolls MR, Voelkel NF. The roles of immunity in the prevention and evolution of pulmonary arterial hypertension. *Am J Respir Crit Care Med* 2017;**195**:1292–1299.
- Swiers G, de Bruijn M, Speck NA. Hematopoietic stem cell emergence in the conceptus and the role of Runx1. *Int J Dev Biol* 2010;**54**:1151–1163.
- Lichtinger M, Ingram R, Hannah R, Muller D, Clarke D, Assi SA, Lie ALM, Noailles L, Vijayabaskar MS, Wu M, Tenen DG, Westhead DR, Kouskoff V, Lacaud G, Gottgens B, Bonifer C. RUNX1 reshapes the epigenetic landscape at the onset of haematopoiesis. *EMBO J* 2012;**31**:4318–4333.
- Chen MJ, Yokomizo T, Zeigler BM, Dzierzak E, Speck NA. Runx1 is required for the endothelial to hematopoietic cell transition but not thereafter. *Nature* 2009;**457**:887–891.
- Levanon D, Groner Y. Structure and regulated expression of mammalian RUNX genes. *Oncogene* 2004;**23**:4211–4219.
- Wang Q, Stacy T, Binder M, Marin-Padilla M, Sharpe AH, Speck NA. Disruption of the Cbfa2 gene causes necrosis and hemorrhaging in the central nervous system and blocks definitive hematopoiesis. *Proc Natl Acad Sci U S A* 1996;**93**:3444–3449.
- Liang OD, So EY, Egan PC, Goldberg LR, Aliotta JM, Wu KQ, Dubielecka PM, Ventetuolo CE, Reginato AM, Quesenberry PJ, Klinger JR. Endothelial to hematopoietic transition contributes to pulmonary arterial hypertension. *Cardiovasc Res* 2017;**113**:1560–1573.
- Mills CD. M1 and M2 macrophages: oracles of health and disease. *Crit Rev Immunol* 2012;**32**:463–488.
- Wu KQ, Muratore CS, So EY, Sun C, Dubielecka PM, Reginato AM, Liang OD. M1 macrophage-induced endothelial-to-mesenchymal transition promotes infantile hemangioma regression. *Am J Pathol* 2017;**187**:2102–2111.
- Luo MC, Zhou SY, Feng DY, Xiao J, Li WY, Xu CD, Wang HY, Zhou T. Runt-related transcription factor 1 (RUNX1) binds to p50 in macrophages and enhances TLR4-triggered inflammation and septic shock. *J Biol Chem* 2016;**291**:22011–22020.
- Tugal D, Liao X, Jain MK. Transcriptional control of macrophage polarization. *Arterioscler Thromb Vasc Biol* 2013;**33**:1135–1144.
- Cunningham L, Finckbeiner S, Hyde RK, Southall N, Marugan J, Yedavalli VR, Dehdashti SJ, Reinhold WC, Alemu L, Zhao L, Yeh JR, Sood R, Pommier Y, Austin CP, Jeang KT, Zheng W, Liu P. Identification of benzodiazepine Ro5-3335 as an inhibitor of CBF leukemia through quantitative high throughput screen against RUNX1-CBFbeta interaction. *Proc Natl Acad Sci U S A* 2012;**109**:14592–14597.
- Klinger JR, Pereira M, Del Totto M, Brodsky AS, Wu KQ, Dooner MS, Borgovan T, Wen S, Goldberg LR, Aliotta JM, Ventetuolo CE, Quesenberry PJ, Liang OD. Mesenchymal stem cell extracellular vesicles reverse Sugen/hypoxia pulmonary hypertension in rats. *Am J Respir Cell Mol Biol* 2020;**62**:577–587.
- Zovein AC, Hofmann JJ, Lynch M, French WJ, Turlo KA, Yang Y, Becker MS, Zanetta L, Dejana E, Gasson JC, Tallquist MD, Iruela-Arispe ML. Fate tracing reveals the endothelial origin of hematopoietic stem cells. *Cell Stem Cell* 2008;**3**:625–636.
- Monvoisin A, Alva JA, Hofmann JJ, Zovein AC, Lane TF, Iruela-Arispe ML. VE-cadherin-CreERT2 transgenic mouse: a model for inducible recombination in the endothelium. *Dev Dyn* 2006;**235**:3413–3422.
- Wang Y, Nakayama M, Pitulescu ME, Schmidt TS, Bochenek ML, Sakakibara A, Adams S, Davy A, Deutsch U, Luthi U, Barberis A, Benjamin LE, Makinen T, Nobes CD, Adams RH. Ephrin-B2 controls VEGF-induced angiogenesis and lymphangiogenesis. *Nature* 2010;**465**:483–486.
- van Beijnum JR, Rousch M, Castermans K, van der Linden E, Griffioen AW. Isolation of endothelial cells from fresh tissues. *Nat Protoc* 2008;**3**:1085–1091.
- Clausen BE, Burkhardt C, Reith W, Renkawitz R, Forster I. Conditional gene targeting in macrophages and granulocytes using LysMcre mice. *Transgenic Res* 1999;**8**:265–277.
- Abram CL, Roberge GL, Hu Y, Lowell CA. Comparative analysis of the efficiency and specificity of myeloid-Cre deleting strains using ROSA-EYFP reporter mice. *J Immunol Methods* 2014;**408**:89–100.
- Damoiseaux JG, Dopp EA, Calame W, Chao D, MacPherson GG, Dijkstra CD. Rat macrophage lysosomal membrane antigen recognized by monoclonal antibody ED1. *Immunology* 1994;**83**:140–147.
- Hu G, Christman JW. Editorial: alveolar macrophages in lung inflammation and resolution. *Front Immunol* 2019;**10**:2275.
- El Chami H, Hassoun PM. Immune and inflammatory mechanisms in pulmonary arterial hypertension. *Prog Cardiovasc Dis* 2012;**55**:218–228.
- Tuder RM, Groves B, Badesch DB, Voelkel NF. Exuberant endothelial cell growth and elements of inflammation are present in plexiform lesions of pulmonary hypertension. *Am J Pathol* 1994;**144**:275–285.
- Sahara M, Sata M, Morita T, Nakamura K, Hirata Y, Nagai R. Diverse contribution of bone marrow-derived cells to vascular remodeling associated with pulmonary arterial hypertension and arterial neointimal formation. *Circulation* 2007;**115**:509–517.
- Burke DL, Frid MG, Kunrath CL, Karoor V, Anwar A, Wagner BD, Strassheim D, Stenmark KR. Sustained hypoxia promotes the development of a pulmonary artery-specific chronic inflammatory microenvironment. *Am J Physiol Lung Cell Mol Physiol* 2009;**297**:L238–250.
- Vergadi E, Chang MS, Lee C, Liang OD, Liu X, Fernandez-Gonzalez A, Mitsialis SA, Kourembanas S. Early macrophage recruitment and alternative activation are critical for the later development of hypoxia-induced pulmonary hypertension. *Circulation* 2011;**123**:1986–1995.
- Savai R, Pullamsetti SS, Kolbe J, Bieniek E, Voswinckel R, Fink L, Scheed A, Ritter C, Dahal BK, Vater A, Klussmann S, Ghofrani HA, Weissmann N, Klepetko W, Banat GA, Seeger W, Grimminger F, Schemmly RT. Immune and inflammatory cell involvement in the pathology of idiopathic pulmonary arterial hypertension. *Am J Respir Crit Care Med* 2012;**186**:897–908.
- Florentin J, Coppin E, Vasamsetti SB, Zhao J, Tai YY, Tang Y, Zhang Y, Watson A, Sembrat J, Rojas M, Vargas SO, Chan SY, Dutta P. Inflammatory macrophage expansion in pulmonary hypertension depends upon mobilization of blood-borne monocytes. *J Immunol* 2018;**200**:3612–3625.
- Tian W, Jiang X, Tamosiuniene R, Sung YK, Qian J, Dhillon G, Gera L, Farkas L, Rabinovitch M, Zamanian RT, Inayathullah M, Fridlib M, Rajadas J, Peters-Golden M, Voelkel NF, Nicolls MR. Blocking macrophage leukotriene b4 prevents endothelial injury and reverses pulmonary hypertension. *Sci Transl Med* 2013;**5**:200ra117.
- Voelkel NF, Peters-Golden M. A new treatment for severe pulmonary arterial hypertension based on an old idea: inhibition of 5-lipoxygenase. *Pulm Circ* 2020;**10**:2045894019882635.
- Trankle CR, Canada JM, Kadariya D, Markley R, De Chazal HM, Pinson J, Fox A, Van Tassel BW, Abbate A, Grinnan D. IL-1 blockade reduces inflammation in pulmonary arterial hypertension and right ventricular failure: a single-arm, open-label, phase IB/II pilot study. *Am J Respir Crit Care Med* 2019;**199**:381–384.
- Hirschi KK. Hemogenic endothelium during development and beyond. *Blood* 2012;**119**:4823–4827.
- Alva JA, Zovein AC, Monvoisin A, Murphy T, Salazar A, Harvey NL, Carmeliet P, Iruela-Arispe ML. VE-Cadherin-Cre-recombinase transgenic mouse: a tool for lineage analysis and gene deletion in endothelial cells. *Dev Dyn* 2006;**235**:759–767.
- Pelosi E, Valtieri M, Coppola S, Botta R, Gabbianelli M, Lulli V, Marziali G, Masella B, Muller R, Sgadari C, Testa U, Bonanno G, Peschle C. Identification of the hemangioblast in postnatal life. *Blood* 2002;**100**:3203–3208.
- Wu X, Lensch MW, Wylie-Sears J, Daley GQ, Bischoff J. Hemogenic endothelial progenitor cells isolated from human umbilical cord blood. *Stem Cells* 2007;**25**:2770–2776.
- Pelosi E, Castelli G, Martin-Padura I, Bordini V, Santoro S, Conigliaro A, Cerio AM, De Santis Puzzonza M, Marighetti P, Biffoni P, Alonzi T, Amicone L, Alcalay M, Bertolini F, Testa U, Tripodi M. Human haemato-endothelial precursors: cord blood CD34+ cells produce haemogenic endothelium. *PLoS One* 2012;**7**:e51109.
- Graf S, Haimel M, Bleda M, Hadinnapola C, Southgate L, Li W, Hodgson J, Liu B, Salmon RM, Southwood M, Machado RD, Martin JM, Treacy CM, Yates K, Daugherty LC, Shamardina O, Whitehorn D, Holden S, Aldred M, Bogaard HJ, Church C, Coghlan G, Condliffe R, Corris PA, Danesino C, Eyries M, Gall H, Ghio S, Ghofrani HA, Gibbs JSR, Girerd B, Houweling AC, Howard L, Humbert M, Kiely DG, Kovacs G, MacKenzie Ross RV, Moledina S, Montani D, Newnham M, Olschewski A, Olschewski H, Peacock AJ, Pepke-Zaba J, Prokopenko I, Rhodes C, Scelsi L, Seeger W, Soubrier F, Stein DF, Suntharalingam J, Swietlik EM, Toshner MR, van Heel DA, Vonk Noordegraaf A, Waisfisz Q, Wharton J, Wort SJ, Ouweland WH, Soranzo N, Lawrie A, Upton PD, Wilkins MR, Trembath RC, Morrell NW. Identification of rare sequence variation underlying heritable pulmonary arterial hypertension. *Nat Commun* 2018;**9**:1416.
- Hiraide T, Kataoka M, Suzuki H, Aimi Y, Chiba T, Kanekura K, Satoh T, Fukuda K, Gamou S, Kosaki K. SOX17 mutations in Japanese patients with pulmonary arterial hypertension. *Am J Respir Crit Care Med* 2018;**198**:1231–1233.

45. Zhu N, Welch CL, Wang J, Allen PM, Gonzaga-Jauregui C, Ma L, King AK, Krishnan U, Rosenzweig EB, Ivy DD, Austin ED, Hamid R, Pauciulo MW, Lutz KA, Nichols WC, Reid JG, Overton JD, Baras A, Dewey FE, Shen Y, Chung WK. Rare variants in SOX17 are associated with pulmonary arterial hypertension with congenital heart disease. *Genome Med* 2018;**10**:56.
46. Rhodes CJ, Batai K, Bleda M, Haimel M, Southgate L, Germain M, Pauciulo MW, Hadinnapola C, Aman J, Girerd B, Arora A, Knight J, Hanscombe KB, Karnes JH, Kaakinen M, Gall H, Ulrich A, Harbaum L, Cebola I, Ferrer J, Lutz K, Swietlik EM, Ahmad F, Amouyel P, Archer SL, Argula R, Austin ED, Badesch D, Bakshi S, Barnett C, Benza R, Bhatt N, Bogaard HJ, Burger CD, Chakinala M, Church C, Coghlan JG, Condliffe R, Corris PA, Danesino C, Debette S, Elliott CG, Elwing J, Eyries M, Fortin T, Franke A, Frantz RP, Frost A, Garcia JGN, Ghio S, Ghofrani HA, Gibbs JSR, Harley J, He H, Hill NS, Hirsch R, Houweling AC, Howard LS, Ivy D, Kiely DG, Klinger J, Kovacs G, Lahm T, Laudes M, Machado RD, Ross RVM, Marsolo K, Martin LJ, Moledina S, Montani D, Nathan SD, Newnham M, Olschewski A, Olschewski H, Oudiz RJ, Ouwehand WH, Peacock AJ, Pepke-Zaba J, Rehman Z, Robbins I, Roden DM, Rosenzweig EB, Saydain G, Scelsi L, Schilz R, Seeger W, Shaffer CM, Simms RW, Simon M, Sitbon O, Suntharalingam J, Tang H, Tchourbanov AY, Thenappan T, Torres F, Toshner MR, Treacy CM, Vonk Noordegraaf A, Waisfisz Q, Walsworth AK, Walter RE, Wharton J, White RJ, Wilt J, Wort SJ, Yung D, Lawrie A, Humbert M, Soubrier F, Tregouet DA, Prokopenko I, Kittles R, Graf S, Nichols WC, Trembath RC, Desai AA, Morrell NW, Wilkins MR; Consortium UNBRD, Consortium UPCS, Consortium UPB. Genetic determinants of risk in pulmonary arterial hypertension: international genome-wide association studies and meta-analysis. *Lancet Respir Med* 2019;**7**:227–238.
47. Zhu N, Swietlik EM, Welch CL, Pauciulo MW, Hagen JJ, Zhou X, Guo Y, Karten J, Pandya D, Tilly T, Lutz KA, Martin JM, Treacy CM, Rosenzweig EB, Krishnan U, Coleman AW, Gonzaga-Jauregui C, Lawrie A, Trembath RC, Wilkins MR, Heritable PAH, Morrell NW, Shen Y, Graf S, Nichols WC, Chung WK; Regeneron Genetics Center, PAH Biobank Enrolling Centers' Investigators, NIH BioResource for Translational Research – Rare Diseases, National Cohort Study of Idiopathic and Heritable PAH. Rare variant analysis of 4241 pulmonary arterial hypertension cases from an international consortium implicates FBLN2, PDGFD, and rare de novo variants in PAH. *Genome Med* 2021;**13**:80.
48. Lizama CO, Hawkins JS, Schmitt CE, Bos FL, Zape JP, Cautivo KM, Borges Pinto H, Rhyner AM, Yu H, Donohoe ME, Wythe JD, Zvein AC. Repression of arterial genes in hemogenic endothelium is sufficient for haematopoietic fate acquisition. *Nat Commun* 2015;**6**:7739.
49. Bos FL, Hawkins JS, Zvein AC. Single-cell resolution of morphological changes in hemogenic endothelium. *Development* 2015;**142**:2719–2724.
50. Zhang L, Jambusaria A, Hong Z, Marsboom G, Toth PT, Herbert BS, Malik AB, Rehman J. SOX17 regulates conversion of human fibroblasts into endothelial cells and erythroblasts by dedifferentiation into CD34(+) progenitor cells. *Circulation* 2017;**135**:2505–2523.
51. Nakajima-Takagi Y, Osawa M, Oshima M, Takagi H, Miyagi S, Endoh M, Endo TA, Takayama N, Eto K, Toyoda T, Koseki H, Nakauchi H, Iwama A. Role of SOX17 in hematopoietic development from human embryonic stem cells. *Blood* 2013;**121**:447–458.
52. Riddell A, McBride M, Braun T, Nicklin SA, Cameron E, Loughrey CM, Martin TP. RUNX1: an emerging therapeutic target for cardiovascular disease. *Cardiovasc Res* 2020;**116**:1410–1423.
53. McCarroll CS, He W, Foote K, Bradley A, McGlynn K, Vidler F, Nixon C, Nather K, Fattah C, Riddell A, Bowman P, Elliott EB, Bell M, Hawksby C, MacKenzie SM, Morrison LJ, Terry A, Blyth K, Smith GL, McBride MW, Kubin T, Braun T, Nicklin SA, Cameron ER, Loughrey CM. Runx1 deficiency protects against adverse cardiac remodeling after myocardial infarction. *Circulation* 2018;**137**:57–70.
54. Li X, Zhang S, Wa M, Liu Z, Hu S. MicroRNA-101 protects against cardiac remodeling following myocardial infarction via downregulation of runt-related transcription factor 1. *J Am Heart Assoc* 2019;**8**:e013112.
55. Koth J, Wang X, Killen AC, Stockdale WT, Potts HG, Jefferson A, Bonkhofer F, Riley PR, Patient RK, Gottgens B, Mommersteeg MTM. Runx1 promotes scar deposition and inhibits myocardial proliferation and survival during zebrafish heart regeneration. *Development* 2020;**147**:dev186569.
56. Lambert M, Jambon S, Depauw S, David-Cordonnier MH. Targeting transcription factors for cancer treatment. *Molecules* 2018;**23**:1479.
57. Haubrich RH, Flexner C, Lederman MM, Hirsch M, Pettinelli CP, Ginsberg R, Lietman P, Hamzeh FM, Spector SA, Richman DD; AIDS Clinical Trials Group 213 Team. A randomized trial of the activity and safety of Ro 24-7429 (Tat antagonist) versus nucleoside for human immunodeficiency virus infection. *J Infect Dis* 1995;**172**:1246–1252.
58. Kira T, Hashimoto K, Baba M, Okamoto T, Shigeta S. 2-Glycineamide-5-chlorophenyl 2-pyrryl ketone, a non-benzodiazepin Tat antagonist, is effective against acute and chronic HIV-1 infections in vitro. *Antiviral Res* 1996;**32**:55–62.
59. Shahabuddin M, Volsky B, Hsu MC, Volsky DJ. Restoration of cell surface CD4 expression in human immunodeficiency virus type 1-infected cells by treatment with a Tat antagonist. *J Virol* 1992;**66**:6802–6805.
60. Lam JD, Oh DJ, Wong LL, Amarnani D, Park-Windhol C, Sanchez AV, Cardona-Velez J, McGuone D, Stemmer-Rachamimov AO, Elliott D, Bielenberg DR, van Zyl T, Shen L, Gai X, D'Amore PA, Kim LA, Arboleda-Velasquez JF. Identification of RUNX1 as a mediator of aberrant retinal angiogenesis. *Diabetes* 2017;**66**:1950–1956.
61. Richter LE, Wang Y, Becker ME, Coburn RA, Williams JT, Amador C, Hyde RK. HDAC1 is a required cofactor of CBFbeta-SMMHC and a potential therapeutic target in inversion 16 acute myeloid leukemia. *Mol Cancer Res* 2019;**17**:1241–1252.
62. Illendula A, Gilmour J, Grembecka J, Tirumala VSS, Boulton A, Kuntimaddi A, Schmidt C, Wang L, Pulikkan JA, Zong H, Parlak M, Kuscu C, Pickin A, Zhou Y, Gao Y, Mishra L, Adli M, Castilla LH, Rajewski RA, Janes KA, Guzman ML, Bonifer C, Bushweller JH. Small molecule inhibitor of CBFbeta-RUNX binding for RUNX transcription factor driven cancers. *EBioMedicine* 2016;**8**:117–131.
63. Illendula A, Pulikkan JA, Zong H, Grembecka J, Xue L, Sen S, Zhou Y, Boulton A, Kuntimaddi A, Gao Y, Rajewski RA, Guzman ML, Castilla LH, Bushweller JH. Chemical biology. A small-molecule inhibitor of the aberrant transcription factor CBFbeta-SMMHC delays leukemia in mice. *Science* 2015;**347**:779–784.

## Translational perspective

RUNX1 inhibition *in vivo* reversed pulmonary hypertension and improved vascular remodelling in the Sugen/hypoxia-induced pulmonary hypertension model in rats. These findings suggest that, by blocking RUNX1-dependent endothelial to haematopoietic transformation and pulmonary macrophage recruitment and activation, targeting RUNX1 may be as a novel treatment modality for pulmonary arterial hypertension.